A New Model of the Acoustic Reflex

A. Longtin and J.-R. Derome

Physics Department, University of Montreal, Montreal, Canada

Abstract. A system-type model of the acoustic reflex in man is proposed with the intention of sheding light on certain of its nonlinear behaviors. This model is the first to incorporate into the multipath structure of the reflex arc the adaptation and recovery processes. Parameter distribution in the parallel pathways is based on the current knowledge on the stapedius muscle and on motoneuron pool organization. A piecewise linear system is used in modeling adaptation at onset and recovery at offset. The model is calibrated at 2000 Hz, a frequency for which all the important parameters are available. Two nonlinear behaviors of the adaptation rate are explained: the frequency and intensity dependence, related respectively to the frequency dependence of the feedback gain and to the sigmoidal shape of the closed-loop stimulus-response curve. Underlying physiological mechanisms are discussed, along with other plausible nonlinear models, and extensions of the model to other stimuli are suggested.

1 Introduction

Ever since its establishment as an efficient diagnostic tool for certain auditory pathologies, the acoustic reflex (AR) has received attention at both the experimental and theoretical levels. It was soon recognized that this relatively simple control system was endowed with several essential nonlinear behaviors, even under normal operating conditions. This fact certainly stunted many efforts directed at a mathematical description of the AR, without hindering the flourishing interest at the experimental level. Nevertheless, a few models have been proposed since the pioneering work of Zwislocki (1960) and they will be reviewed briefly in Sect. 3.

Our model follows the tradition of black-box analyses set forth by the earlier works. However, it stresses the distributed nature of the reflex arc (multi-path structure), an approach whose fertility has been well demonstrated by Borg (1972, 1973a, b). It emphasizes the physiological processes underlying the behavior of the AR response. It also concentrates on two characteristics on which little theoretical work has been done, although the first has been extensively studied clinically: adaptation and recovery. These concepts are crucial in understanding the protection to sustained and intermittent acoustic stimuli offered by the AR. Thus, the elaboration of a mathematical model is justified to test various hypotheses pertaining to the processes involved.

In order to decouple the effects related strictly to adaptation or recovery from those due to other components of the reflex arc, an accurate model is developed which properly accounts for the open-loop and the closed-loop behaviors as summarized in the next section. It is based on the most recent physiological data concerning the reflex arc and also on general studies of neuromuscular systems.

The AR is a negative feedback control system activated by sounds above a certain threshold. Its final effect is the contraction of the middle-ear stapedius muscle (the only one that seems to be activated by sound in man) which modifies the mechanical transfer-function of the middle-ear ossicles. It essentially attenuates low frequency sounds. Its study can benefit from the large body of work on the pupil light reflex, due to the close homomorphism of these systems both structurally and functionally speaking. We shall see that the pupil reflex has the same intensity dependence of its adaptive response (pupillary escape nonlinearity) as does the AR at frequencies below about 3000 Hz. Furthermore, we shall try to explain this dependency as well as the fast recovery in the light shed by models proposed for other adaptive modalities (hair cell adaptation, stretch receptor adaptation, ...).

It should be mentioned that many ideas have been put forward as to the rôle of the AR (see Borg et al.

1984): 1) extension of the dynamic range of the ear; 2) protection of the inner ear (mainly of the hair cells) from damage due to excessive acoustic energies; 3) refinement of the spatial localization of sound sources; 4) minimization of middle-ear resonance effects; 5) discrimination of high frequency sounds, and so on. The first two are generally accepted. While it would be unfair to rebuke the others on the grounds of their "implausibility", we believe that their assertion would require a much finer knowledge of the AR dynamics than is available in the literature. Thus we restrict our attention to the regulatory aspect of the AR.

In Sect. 2 we summarize and evaluate the AR's behaviors pertinent to its mathematical description. Section 3 gives a brief account of the AR modeling efforts to this day, followed by the precise objectives of our proposed model. Next the mathematical description of the sensory and motor processes is presented. Section 4 elaborates the parameter identification scheme. Section 5 reports on the numerical simulations of the AR dynamics under open and closed-loop conditions. Section 6 discusses the model's results as well as its predictions relative to the adaptation and recovery time constants.

2 Acoustic Reflex Behavioral Characteristics

The middle-ear ossicles act as an impedance transformer between two fluids of different densities: the air and the perilymph in the cochlea. It ensures the efficient transfer of acoustic energy at all frequencies. The AR consists in the sound elicited contraction of the stapedius muscle, which pulls on the stapes and stiffens the ossicular chain. The change in impedance results in a decrease of transmission at low frequencies.

The acoustic reflex is bilateral. This enables one to stimulate one ear and monitor the changes in the ear contralateral to the stimulus. In animal experiments, these changes are based on invasive electromyographic techniques or on immittance (impedance or admittance, see ANSI 1982) measurements at the eardrum. In humans, immittance techniques are generally used (cf. Borg 1968; Møller 1961) to measure the ipsi- and contralateral time course of the response. Several studies report admittance changes while others consider impedance changes. According to Borg and Møller (1968), impedance change is a good measure of stapedius tension, since it is proportional to the rectified and integrated electromyogram (EMG) which has been shown to be proportional to tension in an isometric contraction.

While a percent change in admittance is not equivalent to a percent change in impedance (Wilson et al. 1978), both measures yield similar time courses

(see e.g., Antablin et al. 1980) with similar time constants.

A typical response to a rectangular pulse of sound is shown in Fig. 1. At lower stimulus frequencies one can observe damped oscillations at the onset. Let us define the quantities that characterize the time course. The latency time T_{lat} is a measure of the response's delay. When measured by electromyographic means, it is equal to the conduction time in the reflex arc. In the context of immittance measurements, it comprises the additional time for the contraction to produce a noticeable modification of immittance at the eardrum (due to mechanical coupling). This latter value of T_{lat} is the important one regarding the AR dynamics because impedance change is the ultimate feedback signal. Typically, $T_{lat} \sim 100$ ms (2000 Hz).

The initial maximum amplitude of the response A_{imax} is the value of the peak immittance change. It occurs at a time TS, the summation time which is of the order of a second. The rise-time T_{rise} is the interval during which the response climbs from 10% to 90% of A_{imax}.

The definition of adaptation half-life is touchy (see Fig. 1B). Several studies define it as the time for the response to decrease from A_{imax} to 50% A_{imax}. However, assuming adaptation has an exponential time
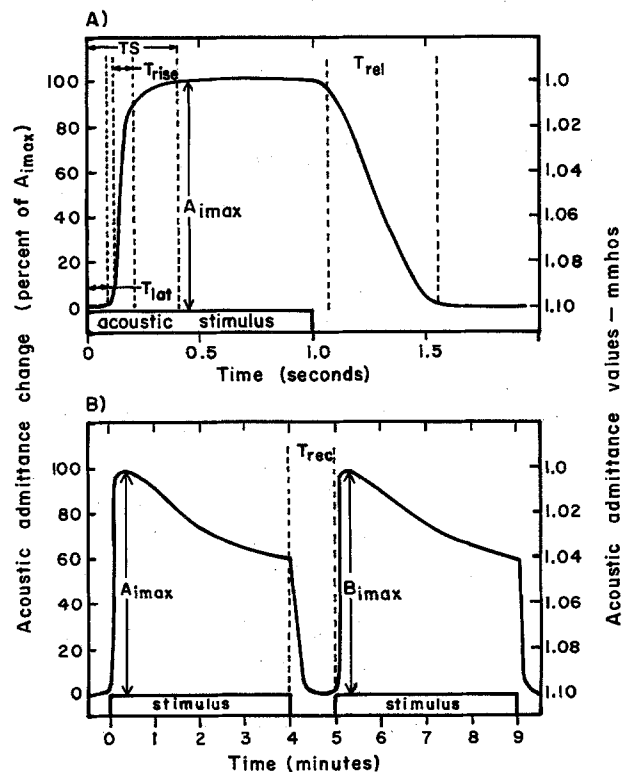

Fig. 1. Typical AR response to a mid frequency contralateral stimulation. Quantities are defined in the text. (From Mayrand 1982)

course (as is done in most studies), this is not the real half-life if the steady-state is not zero. We thus define the real half-life as the time for a drop from A_{imax} to halfway between A_{imax} and the steady-state. If "a" is the steady-state value and "$a+b$" the peak value, the first half-life $t'_{1/2}$ is related to the real half-life $t_{1/2}$ by:

$$\{\ln[2b/(b-a)]\}\, t_{1/2} = t'_{1/2}\ln 2. \tag{1}$$

We shall define the way to measure $t_{1/2}$ in the context of our model in Sect. 4.

T_{rel} is the relaxation time for the response to decrease from 90% to 10% of the level prior to offset. It can be deduced from Borg and Nilsson (1984) that it would be between 100 to 500 ms, making it slower than T_{rise}. This is a typical case of URS (unidirectional rate sensitivity: see Clynes 1962), and is due to the slower process of muscle relaxation and to after-discharge in the efferent arc (Borg 1976).

T_{rec}, the recovery time, is the period of silence required to restore the initial amplitude A_{imax} after the onset of a second pulse. The peak of a second onset is noted B_{imax}.

Next we summarize the variations of some of these quantities for different stimulus conditions. They refer, unless specified, to contralateral admittance change responses; the sound levels refer either to dB hearing threshold SPL or to the acoustic reflex threshold (ART).

2.1 Intensity Dependent Effects

T_{lat} varies inversely with stimulus intensity, and tends to be constant at high intensity. In a 20–25 dB range re:ART, T_{rise} also falls when intensity increases. A_{imax} increases with intensity according to the closed-loop stimulus-response curve (SRC) of Fig. 2. This curve is sigmoidal: it is linear above 10 dB re:ART and saturates between 34 and 50 dB for a broadband noise (BBN) and between 24 and 28 dB for pure tones. Over a 20–30 dB range, there is no correlation between T_{rel} and stimulus intensity.

2.2 Influence of the Temporal Characteristics of the Stimulus

A_{imax} is proportional to stimulus durations when they are shorter than 500 ms. For stimuli longer than a second, A_{imax} remains constant, but a decay sets in, whose rate is frequency dependent (see adaptation). The dependency on stimulus duration is known as temporal summation, to which the psychophysical phenomenon of Bloch's law is related.

2.3 Influence of Stimulus Spectral Characteristics

The ART is nearly constant for pure tones between 500 and 4000 Hz, and is on the average 20 dB lower for a
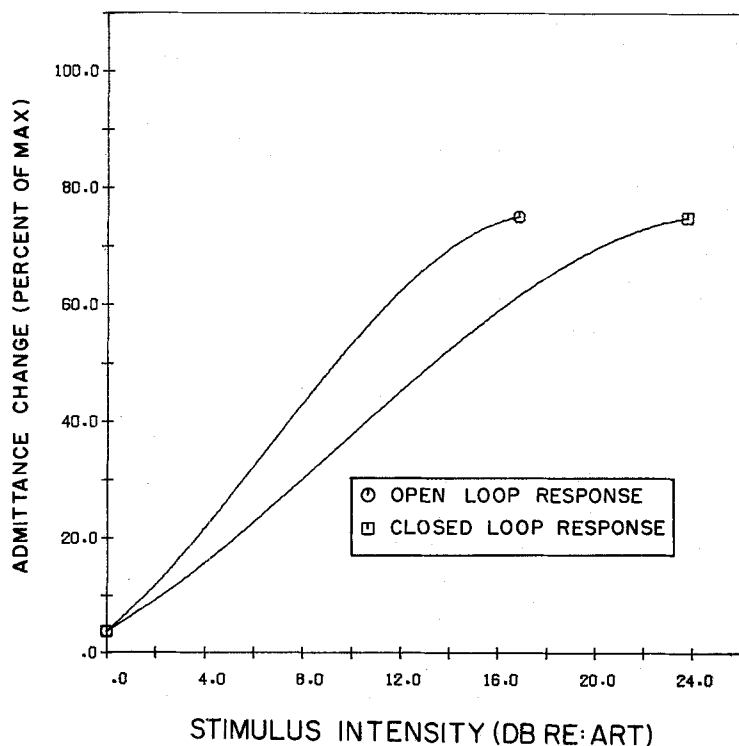

STIMULUS-RESPONSE CURVES AT 2000 Hz

(Graph: ADMITTANCE CHANGE (PERCENT OF MAX) vs STIMULUS INTENSITY (DB RE·ART); legend: ⊙ OPEN LOOP RESPONSE, ▢ CLOSED LOOP RESPONSE)

Fig. 2. Closed-loop SRC (from Wilson and McBride, 1978): $\Delta Y(\%)$
$= 3.706 + 2.546\, I + 0.1358\, I^2 - 0.004913\, I^3$ and open-loop SRC calculated from the CL-SRC assuming a 0.3 dB/dB regulation: $\Delta Y(\%)$
$= 3.706 + 3.639\, I + 0.2771\, I^2 - 0.01432\, I^3$

BBN. This last fact stems certainly from the spatial summation in the afferent pathways up to the stapedius motoneuron pool, because a BBN excites the whole cochlea. In fact, stimulus-tone frequency is hardly encoded at the pool level (Borg 1976) which is in clear contrast with the tuning curves of the primary auditory neurons.

The onset to a low frequency tone (< 800 Hz) causes damped oscillations which are absent at higher frequencies.

2.4 Adaptation and Recovery

The AR cannot maintain a steady response to a prolonged stimulus. It adapts from A_{imax} to an asymptotic value A_∞, exhibiting a fast phase followed by a slow phase. For a BBN, the fast phase lasts about 4 min, with an asymptotic response of 40–50% A_{imax} (Hétu and Carreau 1977). We shall only be interested by the fast phase.

The amount of adaptation is independent of the stimulus level when absolute changes of immittance are considered (Wilson et al. 1978). When responses are expressed as percentage of A_{imax}, adaptation decreases at high intensity for frequencies below 2000 Hz; this means that the ratio of A_{imax} to A_∞ decreases with increasing intensity. Typically (Wilson et al. 1978), for a 10 dB re:ART BBN, $t'_{1/2} = 18.5$ s (standard deviation 13.1).

Above 2000 Hz, the majority of studies report no dependence of adaptation on intensity within a 20 dB range above ART (Silman 1984).

Adaptation is less pronounced as the frequency is lowered. At 2000 Hz, $t'_{1/2} = 14$ s while at 500 Hz it is greater than 31 s (Wilson et al. 1984). The presence of silent intervals inhibits adaptation partly or completely. Measures of this "recovery", characterized by T_{rec}, show large variability because recovery is only asymptotically complete. The time necessary for a 50% recovery $T_{rec}(1/2)$ is more accurate. For a BBN, $T_{rec} \sim 60$ s, while at 2000 Hz it is worth 1–3 s with $T_{rec}(1/2) \sim 250$ ms (Borg and Ödman 1979). Recovery seems to be an exponential function of the duration of the silent interval (Borg and Ödman 1979; Lalande and Hétu 1979).

It is believed (Lutman and Martin 1978) that adaptation, in its fast phase, is not due to stapedius muscle fatigue. In fact, the stapedius is composed mainly of fast resistant (type 2A) muscle fibers (Lyon and Maimgren 1982; Teig and Dahl 1972). Corroborating this assumption is the following experimental evidence: an adapted response can be suddenly "reviewed" by modifying the stimulus frequency, an indication that the stapedius was intact despite adaptation in the afferent pathways specific to the first frequency. The time course suggests a depletion of metabolic reserves in the afferent arc (Lutman and Martin 1978). Other processes can also be responsible (see Sect. 3). The question is still not settled. The same goes for the site of adaptation. The efferent arc is excluded because the process is frequency dependent. It is probably near the superior olivary nucleus (Lutman and Martin 1978). Also unknown is whether the same site governs the recovery process.

2.5 Open-Loop and Closed-Loop

When the feedback loop is closed, the stimulus elicits the contraction of both stapedii, thus attenuating the input to the cochlea. The loop can be opened in a variety of ways. In animals, one can perform a myotomy of the ipsilateral stapedius. In humans, the stapedius can be paralyzed for a few weeks during unilateral Bell's palsy. This permits a comparison on the same subject of closed-loop (CL) and open-loop (OL) response, which is important in view of the high variability of clinical measurements. The loop can also be opened by a high frequency sound at which the feedback gain is very small, or with a very short pulse of sound (< 10 ms) in which case the feedback signal cannot attenuate the input because of the response's delay.

The OL response is slower, never oscillatory, but the intensity dependence of T_{lat} and T_{rise} still exists. A comparison of SRC's in OL and CL for patients with Bell's palsy is given in Borg (1968) (see our Fig. 2). A faster saturation can be seen in CL, due to another nonlinear effect superposed to the normal saturation of the reflex response: a decoupling of the incudo-stapedial joint at very high stapedius tensions.

3 Development of the Model

The neural circuitry of the AR, a knowledge of which is essential if a mathematical model is to bear any resemblance to reality, has been well studied by Borg (1973a) in the rabbit, although the central portions (superior olivary nucleus, etc.) where adaptation is thought to occur, remain quite obscure. The direct ipsilateral pathways comprise 3 or 4 neurons, the contralateral one always 4. Besides other indirect polysynaptic pathways, there exist many entry points to the reflex arc through which the central nervous system (CNS) can influence the AR response.

It comes as no surprise that the first models of the AR proceeded from linear system analysis since that was the approach used to model the middle-ear. Møller (1961) was probably the first to study the

stapedius reflex from an impedance point of view by incorporating the stiffened muscle into the middle-ear circuit. He also calculated (Møller 1962) the closed-loop transfer function of the AR relating impedance change to sound pressure at different stimulus frequencies. He concluded that, at a given intensity and frequency, the AR acted as a lowpass filter with a cutoff frequency around 5 Hz, and that the oscillations at onset were due to the high feedback gain at low frequencies.

Dallos (1964) arrived at the same result for a 110 dB BBN. He derived a piecewise linear model to account for the URS displayed by the AR in the asymmetry of the speed of the onset and offset responses. By using external feedback. He rendered the system oscillatory and showed the asymmetry of the limit cycle in the phase plane.

Dallos (1973) proposed another model taking into account the threshold nonlinearity and the intensity dependence of the response, both of which he incorporated into the muscle dynamics. His simulations reproduced well the AR nonlinearities, although he neglected a few processes in the reflex arc such as temporal summation, pool of motor units, ...

Borg (1973b) remarked that the AR nonlinearities were common to many polysynaptic somatomotor reflexes. He developed a model of such a reflex and applied it to the study of the AR in the rabbit. It accounted for the onset-offset asymmetry and the intensity dependence of T_{lat} and T_{rise} in open and closed-loop. Thirty "reflex units" (a reflex unit encompassing properties of the muscle fibers, motoneurons and interneurons) of differing characteristics were arranged in a parallel path configuration thus doing justice to the neuroanatomy and neurophysiology of the AR. The model included slow and fast twitch as well as phasic units. The input signal they received was filtered by the temporal summation, a process long known to operate in the afferent arc, and first modeled by Zwislocki (1960) as a low pass first order system with a 200 ms time constant.

To best approximate the OL response, the higher threshold units, which were either of the fast twitch or partly of the phasic type, had shorter time constants than the low threshold slow twitch units (with a gaussian distribution of thresholds amongst the units). This organization is known to occur in motor unit pools according to the "size principle", a term coined by Henneman (Henneman et al. 1965).

Borg's model is again piecewise linear. It does not include the adaptation and recovery processes. Moreover, the units are recruited in an all-or-none fashion, a hypothesis he remarks is valid if the firing rate of the units can be regarded constant in the major part of the dynamic range.

According to Zwislocki (1960), adaptation has a strong influence on temporal summation. He cleverly interrelates both in his model. The excitation brought by an action potential tapers off exponentially; thus temporal summation is accomplished by an imperfect integrator (or leaky integrator: see Inbar and Ginat 1983; Holden 1976). Furthermore, the initial strength of an excitation decreases with the number of action potentials generated. This form of adaptation is of the gain control type (see e.g. Zeevi and Bruckstein 1981).

Tietze (1969a) obtained an equation describing the onset and adaptation, and formulated an electrical model of the process (1969b) in which the response appears as the sum of two exponentials. This model fitted well the data for times less than about 50 s (Wilson et al. 1978), but predicts wrongly a null asymptotic activity.

3.1 Objectives of the Model

We wish to incorporate into a model of the type Borg proposed the most recent physiological data concerning the stapedius and the organization of neuromuscular system in general in order to properly simulate the recruitement of the motor units in OL and CL. We then wish to incorporate the adaptation and recovery processes to study their effect on the AR dynamics as well as their nonlinearities.

Evidently, we must restrict ourselves to one stimulus composition. We shall choose 2000 Hz for the following reasons: 1) the OL and CL responses are known (Borg 1968); 2) adaptation has a relatively short half-life (10–20 s), an important factor for computer time; 3) adaptation does not vary with intensity, thus suggesting an intensity independent time constant; 4) the recovery process has been studied [250 ms half-life, according to Borg and Ödman (1979)]. It will be interesting to suggest how to extend our model to other stimuli. Throughout our model the frequency of action potentials will be considered the important analog quantity; we shall not study the effect of individual action potentials.

3.2 Neural Transduction and Temporal Summation

We shall assume, as Borg did, that the input to the cochlea is already in decibels, even though logarithmic compression occurs in the inner ear. We then consider the effect of the stapedius contraction as a summation (negative) in log units instead of a multiplication. Also the mechanical to neural transduction occuring in the cochlea is considered to be mediated by a linear high pass system; we thus neglect the rectifying effects of the hair cells, their sigmoidal SRC, their very fast adaptation (see Smith and Brachman 1982), etc. Temporal

summation is identical to the one in Borg's model. It is a leaky integrator with a 200 ms time constant which filters any incoming neural signal of any intensity. The step response of this unit gain first order filter is (a step corresponding to a unit value of action potential frequency in arbitrary units):

$$U_{sum}(t) = 1 - \exp(-t/a), \tag{2}$$

where $a = 0.2$.

The transfer function is:

$$H_{sum}(s) = 1/(s + 1/a). \tag{3}$$

3.3 Model of Adaptation and Recovery Processes

Three parameters determine the adaptive response: 1) the rate at onset; 2) the asymptotic value A_∞; 3) the rate of recovery at offset. From Wilson et al. (1984) we can estimate $A_\infty = 0.25 \, A_{imax}$, $T_{rec}(1/2) = 250$ ms and $t'_{1/2} = 14$ s. Knowing A_∞ we can deduce the real half-life from (1):$t_{1/2} = 8.8$ s (or a time constant $\tau = 12.7$ s).

We may first try to formulate a model which would produce both the adaptation and recovery characteristics depending on the value of the input. Although we have chosen the temporal summation to precede adaptation, their order would be irrelevant if both are linear systems. The model must somehow be normalized so as to preserve the units of the output of the temporal summation process. For example, if the input is 10 dB, the steady-state output of the summation is also 10 dB; after one half-life the output should equal 6.25 (half-way between 25% and 100% of 10). The reason motivating this normalization is that we want to calibrate the motor units of the stapedius according to the SRC relating decibels to immittance change (Sect. 4).

It is known that cochlear neurons exhibit a two phase adaptation; the rapid phase lasts a few milliseconds and the slow phase about 40 ms (Smith and Brachman 1982). Duifhuis and Bezemer (1983) have given a summary of multiplicative (gain control) and additive (feedback) models of adaptation in these neurons. In these, the ratio $A(0)/A(\infty)$ of the onset and asymptotic activities increases with intensity, which means more adaptation at high intensity, a behavior opposite to that of the AR below 2000 Hz. Eggermont's stochastic model of this process (1975) and Schroeder and Hall's (1974) synaptic depletion model (of the gain control type) also feature the opposite behavior. These models were only for the slow phase: the former has an intensity independent time constant, but not the latter. They also account for other characteristics: sudden rise in the neuron activity at onset and a nonzero steady-state. More recently, Zeevi and Bruckstein (1981) proposed a model to account for two phase adaptation

in the stretch receptor of the crayfish. The slow phase time constant increased while the fast phase one decreased, like for the AR below 2000 Hz. They hypothesized that a linear negative feedback system, identified with a self-inhibitory current, is responsible for the slow phase, while an adaptive threshold (automatic gain control) accounts for the fast phase. Their hybrid model unfortunately does not reproduce the correct variation of $A(0)/A(\infty)$, which would have been useful for the AR model.

But since we are working at 2000 Hz, with an intensity independent ratio, and since even the fast phase of the AR adaptation is comparatively slow, it is tempting to use their linear slow phase model.

Adaptation of the pupillary light reflex exhibits static and dynamic behaviors quite similar to those of the AR. For instance the response to a small step of light adapts rapidly, a phenomenon termed "pupillary escape"; the response adapts very slowly to a strong light step: this is "pupillary capture" (Semmlow and Chen 1977). Thus the ratio $A(0)/A(\infty)$ shows the same intensity nonlinearity as for the AR. A linear model has been proposed by Stark (1959). His transfer function is of the "leadlag" type as is the one of Zeevi and Bruckstein (1981), although the latter was derived in a less ad hoc fashion.

The use of this linear process for the AR has a serious drawback: the offset response. Equal discontinuities in the input appear as equal discontinuities (with the same sign) in the output, and the output of the process is zero for a null input. Thus negative values can arise at offset, which precludes any identification with action potential frequency. Also, in the absence of any input, the output shows generally a spontaneous (noisy) activity. At offset, the activity is depressed below the noise level, and then recovers to the level prior to onset (see e.g. Schroeder and Hall 1974; Duifhuis and Bezemer 1983). We have been unable to find any evidence that this is the case for the neurons involved in AR adaptation. It has been reported (Fisch and Schulthess 1963) that noise does exist in the arc, which could be related to a resting tonus in the stapedius. One must carefully justify a linear additive adaptation model.

Another point of interest is the rate of recovery; in all the models quoted here, recovery was much slower than adaptation (except for the linear models where the rates are equal). In the AR, we know that recovery time is about two orders of magnitude faster than adaptation time.

We prefer to choose a simple linear process as Stark (1959) and Zeevi and Bruckstein (1981) have done. We will assign a different time constant (independent of the intensity) for onset and offset. The ratio $A(0)/A(\infty)$ is constant, conforming to most reports at 2000 Hz in a
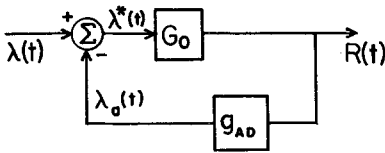
Fig. 3. Linear model of adaptation (Zeevi and Bruckstein 1981)

limited intensity range; the spontaneous value is zero and there is a negative undershoot at offset. We adopt the notation of Zeevi and Bruckstein (1981) (see Fig. 3) (λ is the firing rate):

$$\lambda^*(t) = \lambda(t) - g_{AD}[R(t), \tau_a] \qquad (4)$$

$$= \lambda(t) - \lambda_a(t) \qquad \lambda_a(t) < \lambda(t)$$

$$= 0 \qquad \lambda_a(t) \geqq \lambda(t), \qquad (5)$$

$$\tau_a \dot{\lambda}_a + \lambda_a = MR(t), \qquad (6)$$

$$R(t) = G_0 \lambda^*(t). \qquad (7)$$

The transfer function is

$$H_{ad}(s) = G_0(1 + \tau_a s)/(1 + MG_0 + \tau_a s). \qquad (8)$$

The response to a pulse of duration x is

$$R(t) = F(t)U(t) - F(t - x)U(t - x), \qquad (9)$$

where $U(t)$ is Heaviside's function and where

$$F(t) = G_0 \lambda_0 (1 + MG_0)^{-1} \{1 - \exp[-t(1 + MG_0)/\tau_a]\}$$
$$+ G_0 \lambda_0 \exp[-t(1 + MG_0)/\tau_a]. \qquad (10)$$

Also

$$A(0)/A(\infty) = 1 + MG_0 \qquad (11)$$

(independent of λ).

Defining $P_1 = \tau_a$ and $P_2 = \tau_a/(1 + MG_0)$ we write:

$$P_1 = kF_{on\ off} + P_{1\ (off)}, \qquad (12)$$

where

$$F_{on\ off} = 1 \quad \text{onset}$$

$$= 0 \quad \text{offset}.$$

Values of k and $P_{1\ (off)}$ will be calculated in Sect. 4.

3.4 Model of the Stapedius Neuromuscular System

3.4.1 Properties of the Stapedius (ST).
The human stapedius is a penniform skeletal muscle measuring 6–7 mm in length (the smallest in the human body). The nerve fiber diameter distribution is nearly exponential (Blevins 1968). The histogram of motor unit (MU) diameters in man has not been published to our knowledge. In view of Henneman's "size principle" (1965, 1981), according to which a small nerve fiber innervates a small motor unit having a slow and weak

contraction and a low recruitment threshold and tetanus-twitch ratio, we expect this histogram to be similar to the one for nerve fibers.

About 250 nerve fibers innervate some 1000 muscle fibers (Blevins 1967). The proportion of sensory fibers is not known, and the same can be said for the presence of spindles. We will therefore neglect proprioception. Supposing however that half the fibers are sensory this gives an innervation ratio of about 1 to 7, with approximately 160 MUs. The cat stapedius (ST) is quite similar to man's (Blevins 1964, 1967) and we will use the abundant data on it for our model.

The ST contraction is isometric (Teig 1972a) with a tetanus of 13.9 g in the cat and 15.4 g in the rabbit. We will suppose the tetanus to be 20 g in man, that the MU twitches are distributed (like in the cat) exponentially between 10 and 200 ms (Teig 1972b) and the contraction times between 10 and 50 ms (Teig reports values between 14 and 39 ms in the cat). We thus attribute a slightly stronger force to the human ST, and as long as the absolute values of twitch and tetanus tensions are coherent among themselves, they should yield reasonable responses when expressed in relative units.

We consider only twitch contractions (those involving the propagation of an action potential on the sarcolemma). We neglect phasic contractions (in which the tension eventually goes to zero even with a sustained firing rate in the motoneuron or at its input) because 1) Borg has shown that the AR nonlinearities can be reproduced without them; 2) we want to decouple the effects of AR adaptation and of stapedius fatigue to study adaptation; 3) the models which we shall refer to comprise only twitch contracting units; 4) as we have seen in Sect. 2, there is a predominance of fast fatigue resistant fibers in the cat ST. Teig (1972b) also has reported tetanus-twitch ratios between 2.8 and 4.2 in the cat.

3.4.2 Organization of Motoneuron Pool and Motor Units.
Important facts on the organization of motoneuron pools are revealed in the study by Milner-Brown et al. (1973) of the fast isometric contractions of the first dorsal interosseous (FDI) muscle of the hand. The total muscle tension F_{ti} at which the ith MU is recruited depends linearly on its twitch tension g_i. At high input levels to the pool, tension is increased not by recruitment but by rate-coding.

We assume the ST neuromuscular system to obey rigidly the size principle and the Milner-Brown et al. relations, as has done Christakos (1982a, b) for the FDI. To facilitate numerical simulations, we group the fibers by four, reducing their number to 40, and distribute their tensions exponentially (cf. Milner-Brown et al. 1973) in the interval [10, 200] mg according to the simple rule: the relative frequency of a

tension value is halved for every 40 mg increase. Normalizing the relative frequency distribution so that its integral over the tension interval equals 40, we obtain the number of fibers giving tensions less than or equal to g and more than 10 mg:

$$N(g) = 49.4[e^{-0.173} - e^{-17.3g}].\qquad(13)$$

Inverting this relation gives the value of g_i for $1 \leq i \leq 40$. These values, multiplied by 4 because of the grouping, appear in Table 1 along with other values to be calculated.

We assume like Christakos (1982b) that: 1) the units are independently activated; 2) at a given tension the number of active MUs and the average action potential frequencies are constant, and that the length and speed of the fibers vary very little around their nominal values; 3) the tension can vary from minimal to moderately high; 4) the last MU recruits at 75% of the tetanus tension (15 g in our case). The contraction time γ_i(s) of a twitch is given by (Christakos 1982b):

$$\gamma_i = 0.0478 - 0.0322 \log_{10}[18.75\, g_i].\qquad(14)$$

They appear in Table 1. The first two constants in this relation are calculated from γ_{imin} and γ_{imax} and 18.75 is the slope of the linear equation relating MU twitch tension to MU recruitment level: $F_{ti} = Bg_i$. B is

Table 1. Stapedius motor units. OL and CL refer to open-loop and closed-loop respectively. CT is the contraction time and TTR is the tetanus-twitch ratio. See text for the detail of calculations

Fiber No.	Twitch mg	F-recruit. % F_{max}	I-rec (OL) dB re:ART	I-rec (CL) dB re:ART	ω rad/s	CT ms	S g/dB	TTR —
1	45.6	4.28	0.153	0.220	18.8	50.0	0.743	2.41
2	51.4	4.82	0.301	0.428	19.4	48.3	0.775	2.14
3	57.3	5.37	0.443	0.636	20.0	46.8	0.770	1.99
4	63.4	5.94	0.591	0.842	20.7	45.4	0.807	1.85
5	69.6	6.53	0.736	1.05	21.3	44.1	0.812	1.74
6	76.1	7.13	0.885	1.26	21.9	42.8	0.827	1.63
7	82.7	7.75	1.04	1.47	22.5	41.7	0.840	1.52
8	89.4	8.38	1.18	1.67	23.1	40.6	0.852	1.48
9	96.4	9.04	1.34	1.91	23.7	39.5	0.846	1.37
10	104	9.75	1.50	2.14	24.4	38.5	0.906	1.39
11	111	10.4	1.66	2.36	24.9	37.5	0.894	1.30
12	119	11.2	1.82	2.59	25.6	36.6	0.893	1.26
13	127	11.9	1.98	2.83	26.3	35.7	0.928	1.21
14	135	12.7	2.15	3.07	27.0	34.8	0.941	1.18
15	144	13.5	2.32	3.32	27.7	33.9	0.938	1.16
16	152	14.3	2.50	3.57	28.3	33.2	0.967	1.14
17	162	15.2	2.68	3.83	29.0	32.3	0.952	1.11
18	171	16.0	2.87	4.09	29.8	31.5	0.979	1.10
19	181	17.0	3.06	4.35	30.6	30.7	1.00	1.08
20	192	18.0	3.25	4.65	31.4	29.9	1.01	1.07
21	203	19.0	3.46	4.94	32.2	29.1	1.01	1.07
22	214	20.1	3.67	5.25	33.0	28.4	1.02	1.05
23	226	21.2	3.89	5.56	34.0	27.6	1.03	1.06
24	239	22.4	4.13	5.89	35.0	26.8	1.05	1.07
25	253	23.7	4.37	6.24	35.9	26.0	1.05	1.07
26	267	25.0	4.63	6.61	37.1	25.3	1.06	1.08
27	283	26.5	4.90	7.00	38.3	24.5	1.06	1.09
28	299	28.0	5.19	7.41	39.6	23.7	1.08	1.12
29	317	29.7	5.50	7.85	41.0	22.9	1.09	1.14
30	336	31.5	5.83	8.33	42.4	22.1	1.08	1.17
31	357	33.5	6.19	8.85	44.0	21.2	1.09	1.21
32	380	35.6	6.59	9.42	46.0	20.3	1.08	1.26
33	406	38.1	7.04	10.1	48.1	19.4	1.08	1.33
34	434	40.7	7.53	10.8	50.7	18.5	1.07	1.42
35	467	43.8	8.11	11.6	53.6	17.5	1.05	1.54
36	505	47.3	8.79	12.6	57.2	16.4	1.02	1.71
37	551	51.7	9.64	13.8	61.7	15.1	0.961	1.94
38	609	57.1	10.8	15.4	68.0	13.7	0.857	2.37
39	685	64.2	12.4	17.8	76.9	12.1	0.508	3.14
40	800	75.0	16.7	23.8	93.8	9.9	0.500	4.00

calculated knowing that $F_{t40} = Bg_{40} = B(0.8) = 15$ g, and this permits us to calculate the recruitment level of each MU (see Table 1). Notice that the recruitment level of the first MU is nonzero; we must assume that there is a rest tension not accounted for by the 40 fibers of the model.

3.4.3 Dynamics of Muscle Contraction.

The twitch response has been shown to resemble the impulse response of a second order system at a given firing rate and length (Christakos 1982a). Inbar and Ginat (1983) derive a third order transfer function for the twitch by making explicit the muscle's mechanical components. The internal force generating process is assumed to be second order. Of the global process this can also be true if one neglects tendon filtering and considers only deviations from a rest tension in an isometric contraction. We thus express the twitch response of a MU in the Laplace domain as:

$$\mathscr{L}[g_i(t)] = K_i/(s^2 + 2\xi_i s + \omega_i^2) \tag{15}$$

(K_i constant of the ith MU).

$$g_i(t) = (K_i/2\omega_i \Gamma_i)\{\exp - \omega_i t(\xi_i - \Gamma_i) \\ - \exp - \omega_i t(\xi_i + \Gamma_i)\}, \tag{16}$$

where $\Gamma_i = (\xi_i^2 - 1)^{1/2}$. The contraction time is given by

$$\gamma_i = (1/2\omega_i \Gamma_i) \ln\{(\xi_i + \Gamma_i)/(\xi_i - \Gamma_i)\}. \tag{17}$$

Christakos (1982b) simulates contraction by calculating the effect of each action potential. However, in a model with feedback, it is preferable to consider the analog value of firing frequency and thus to simulate contraction by the response to a step of that frequency value. We shall also consider the response linear (ξ and ω independent of firing rate). The response to a firing rate λ_i step is

$$G_i(t) = \{\lambda_i K_i/2\omega_i^2 \Gamma_i(\Gamma_i - \xi_i)\} [\exp - \omega_i t(\xi_i - \Gamma_i) - 1] \\ + \{\lambda_i K_i/2\omega_i^2 \Gamma_i(\Gamma_i + \xi_i)\} [\exp - \omega_i t(\xi_i + \Gamma_i) - 1]. \tag{18}$$

We next establish the importance of rate-coding in our model. Borg (1973b) chose to neglect rate-coding altogether, while Christakos (1982b) used a linear variation of firing rate with total muscle tension. It is known that MUs recruit and saturate, but little knowledge on rate-coding properties is available. We propose that a MU increases its tension linearly with increasing input, and that it saturates at the recruitment level of the next MU. This "staircase recruitment" approach probably does not do justice to the real system, but it is intermediate between those of Borg and Christakos, and it can easily accommodate new data on rate-coding.

S_i is defined as the rate-coding in g/dB. It is the ratio DT_i/D_i; DT_i is the tension unit (i) must produce to recruit unit ($i+1$) and it is equal to $F_{i+1} - F_i$, where F_i is the recruitment level in grams; D_i is the corresponding input increase in dB equal to $I_{i+1} - I_i$, I being the recruitment level in decibels.

In the next section we determine the remaining model parameters and convert the recruitment levels from grams to decibels.

4 Calibration and Parameter Identification

Figure 4 shows our model in block-diagram form. The graph inside each block represents the step response or the static characteristic of the process. The 40 MUs are organized in the parameter distributed parallel pathway configuration at the output of the adaptation-recovery processes. Tension is applied to the stapes after a delay τ_D and multiplication by the feedback gain.

A value of 75 ms is assigned to τ_D, which is slightly inferior to the shortest latency time observed at 2000 Hz (cf. Silman 1984). It is obtained at high intensity where the contraction is the fastest. It does not comprise contraction time which is handled by the model of the ST.

To simulate the URS manifested by the slower offset, the ω_i values at onset are worth three times their offset values (cf. Dallos' transfer functions 1964).

Feedback gain is forced to zero at offset, because the system must return to the resting state without any influence of ST tension. If the gain were not zero at offset, input would be negative instead of zero, which would incorrectly accelerate the offset.

4.1 Open-Loop Calibration of the Stapedius

The Milner-Brown et al. (1973) relation specifies that a MU recruits when the total muscle tension has reached a certain value. This empirical relation is valid mathematically, but it is not causal physiologically because a MU recruits only when the input to its motoneuron has reached a certain value. In order to preserve this relation, we must convert total muscle tension to stimulus input in decibels which is directly related to motoneuron units. This is done via the SRC at 2000 Hz. We neglect adaptation and temporal summation in the calibration because of their small effect on A_{imax} (see Sect. 4.3).

The closed-loop SRC is useless because we would have to find a way of writing the peak output A_{imax} as a function of the input, and this would obviously require a knowledge of MU recruitment and saturation values, which is the initial problem. A further complication is
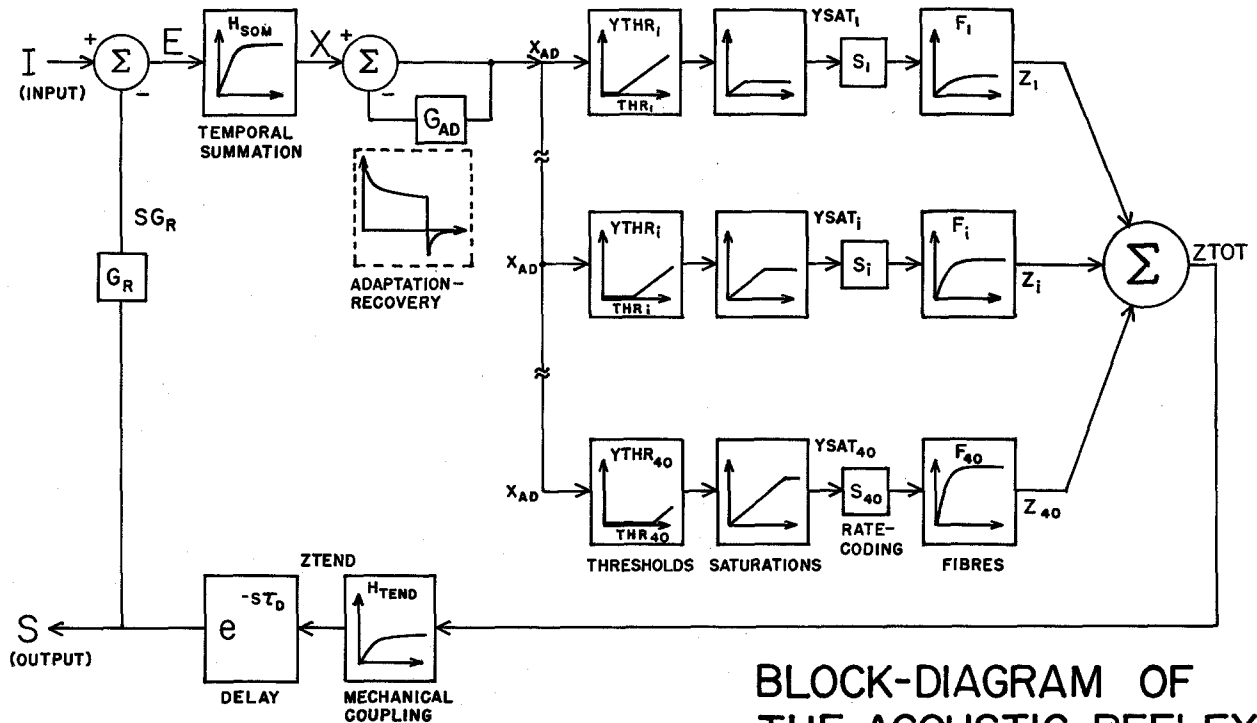
332

Fig. 4. Block diagram of the acoustic reflex

BLOCK-DIAGRAM OF THE ACOUSTIC REFLEX

the presence of feedback: the input to each MU is dependent upon the output of all of them.

In order to calibrate the recruitment levels in decibels, we suggest to use the open-loop SRC which can be calculated from Borg's (1968) study of patients with Bell's palsy. The OL-SRC is higher than the CL-SRC (see Fig. 2). Attenuation is a measure of the horizontal distance between the two curves. If attenuation increases linearly with intensity, we say that the regulation expressed in dB attenuation per dB increase in intensity, is constant. Linear feedback systems obviously exhibit a constant regulation, but this can also be the case for certain ranges of input in nonlinear systems (for which the SRCs are nonlinear). This is the case for the AR in a range greater than 20 dB. At 2000 Hz, the data of Borg (1968, 1971) shows a 0.2–0.3 dB/dB regulation at 2000 Hz, while it is 0.6–0.7 dB/dB at 500 Hz. We use the value of 0.3 dB/dB at 2000 Hz to calculate the open-loop SRC from the closed-loop SRC of Wilson and McBride (1978) obtained with a 660 Hz probe tone (which is close to the 800 Hz tone used by Borg (1968) and by Borg and Ödman (1979) for the study of recovery).

The CL-SRC and the calculated OL-SRC appear in Fig. 2. In CL, the stimulus varies from 0 to 24 dB corresponding to a response of 0 to 75% of the maximal obtainable response. In OL, the same range of response is covered for inputs between 0 and

16.6 dB. The response above 75% is uninteresting because of the incudostapedial joint nonlinearity and because Borg and Ödman (1979) study adaptation and recovery with $A_{imax} = 75\%$ at 2000 Hz. It is also the tension at which the last MU is recruited in our model. In fact, knowing the SRC in OL and CL, it is possible to calculate the recruitment levels in decibels by identifying the 75% response with the 15 g tension.

These values are shown in Table 1, along with the rate-coding values S_i which can also be calculated. The last column contains the tetanus-twitch ratios varying between 1 and 4, which is acceptable in view of Teig's data (1972b). The ST calibration produces the OL-SRC of Fig. 5. It is a piecewise linearization of the calculated one in Fig. 2. This is apparent only at high intensity, e.g. when the 39th unit recruits at 64.2% and increases its tension linearly thereafter.

4.2 Feedback Gain

Mainly because of the incudostapedial joint nonlinearity the feedback gain can be assumed constant only in a 25 dB range (where regulation is constant). We simulate the CL response at a given intensity with different gains and converge on the value producing the proper attenuation at that intensity. A gain of 0.49 produced a 75% response with a 24 dB input. Keeping this value, we can reproduce the whole closed-loop SRC with less
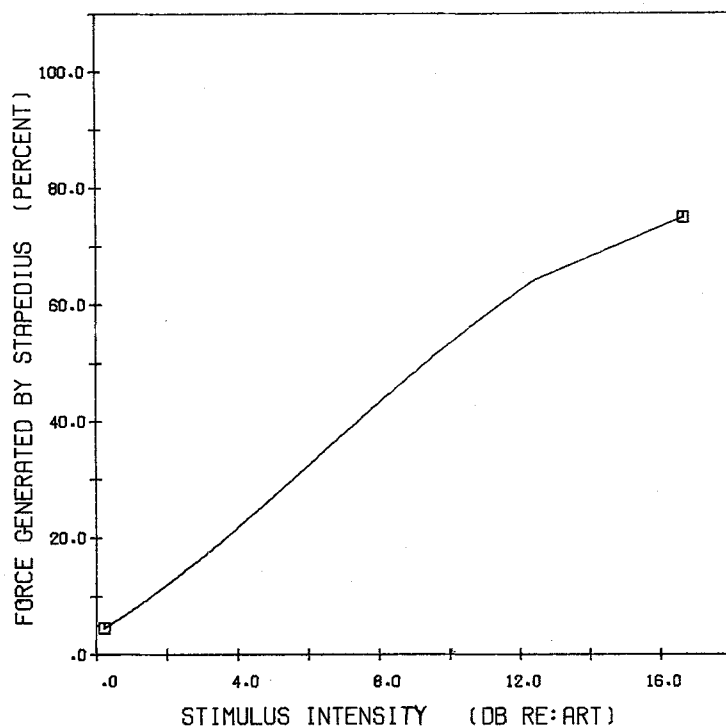
LINEARIZED SRC IN OPEN-LOOP AT 2000 HZ

Fig. 5. Linearized stimulus-response curve (SRC) in open-loop obtained by calibration of the stapedius motor units. The stimulus intensity is given in dB, relative to the acoustic reflex threshold

than a 4% error, demonstrating the coherence of our constant gain calibration of the ST.

4.3 Calibration of Adaptation Processes

The model should produce a ratio $A(0)/A(\infty) = 4$ with $\tau_a = 12.7$ s. Using (11) we can simulate the response with $MG_0 = 3$. Simulations (see Sect. 5) reveal that, in open loop, the response does exhibit these characteristics; however in closed-loop the ratio is less than 4 and $\tau_a > 12.7$. The effect is illustrated with different parameters in Fig. 7. *Negative feedback increases the time constant of adaptation.* To substantiate this effect, we refer to the simpler system of Fig. 6, comprising the adaptation process alone with a forward gain C, representing the static behavior of the ST, and a feedback gain $G = 0.49$. The response to a step E is:

$$y(t) = [EC/(1 + GC)]$$
$$\cdot \{1 - \exp[-t(1 + GC)/(P_2 + GCP_1)]\}$$
$$+ [ECP_1/(P_2 + GCP_1)]$$
$$\cdot \exp[-t(1 + GC)/(P_2 + GCP_1)]. \quad (19)$$

Since we have chosen $P_2 < P_1 (P_1 = \tau_a, P_2 = \tau_a/(1 + MG_0))$ the CL time constant $\tau_{CL} = (P_2 + GCP_1)/(1 + GC)$ is greater than the OL one (P_2), and also $y(0)/y(\infty) = P_1(1 + GC)/(P_2 + GCP_1)$ is less than the OL ratio P_1/P_2.
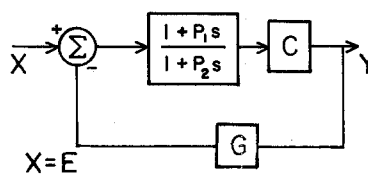

Fig. 6. Feedback system with leadlag adaptation, direct gain and feedback gain

Having analytically justified the increase of τ_a in CL, it remains to find the right τ_a to produce a 12.7 s time constant in CL. We can solve for $\tau_{CL} = 12.7$ and $y(0)/y(\infty) = 4$; the solution is $P_1 = 50.8$ s and $P_2 = 12.7$–38.1 (GC). The constant C simulates the average slope of the ST SRC in OL. To evaluate it, we consider a 10 dB step, for which $A_{imax} = 37.8\%$ in CL, corresponding to 7.57 g. The steady-state value should be 4 times smaller: 1.89 g. From (19): $y(\infty) = 1.89 = 10$ $C/(1 + GC)$ yielding $C = 0.21$, and $P_2 = 8.78$ s, $MG_0 = 4.79$. This means that in OL, τ_a should equal 8.78 s (or $t_{1/2} = 6.1$ s) with $y(0)/y(\infty) = 5.79$.

Figure 7 shows the response of the circuit in Fig. 6 to 7 dB in OL and 10 dB in CL (each yielding $A_{imax} = 37.8\%$ without temporal summation). We see that the summation reduces A_{imax} by about 5% (e.g. to 35.7 in CL), but it does not alter the adaptation time
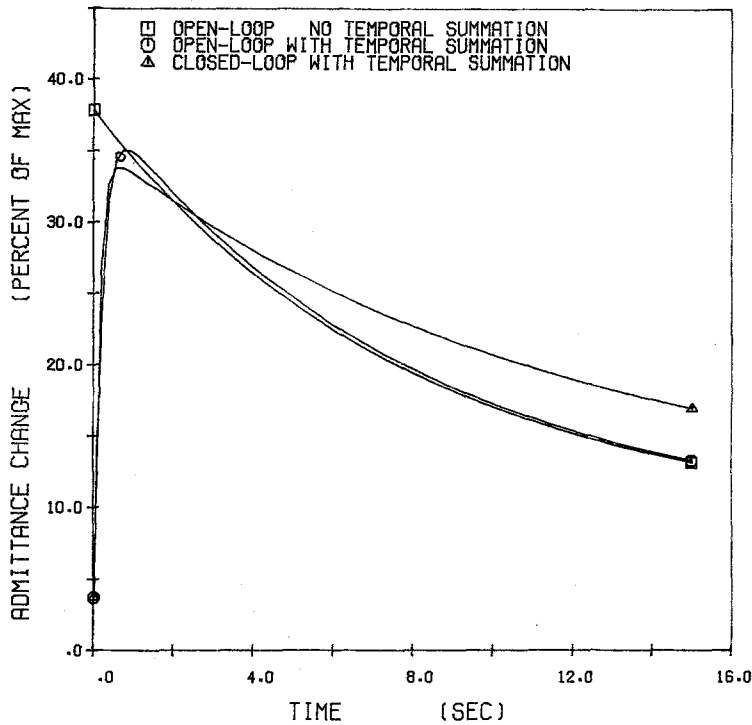
Fig. 7. Step response of the circuit of Fig. 6 in open-loop, with and without temporal summation, and in closed-loop with temporal summation

constant significantly. The small reduction of A_{imax} justifies our neglect of temporal summation in the calibration of the ST in OL and CL.

For these reasons we will assume in the following that A_{imax} occurs at $t = 0$ (like in the absence of temporal summation) and thus we will measure half-life from $t = 0$ (we neglect τ_p). Of course this is for mathematical rigor, and it is not practical in experiments because one cannot infer $A_{imax} = 37.8\%$ from a measurement of 35.7%.

Returning to Fig. 7, we find that the $y(0)/y(\infty)$ ratios and time constants are as predicted, in OL as in CL. The next step is to incorporate this "calibrated adaptation" in the system containing the real ST with the sigmoidal SRC instead of the constant C which only scaled the adaptation output. It should be obvious that an exponential adaptation seen through this SRC now has nothing of an exponential.

To calculate the time course of the adaptation process itself, we must deduce its output by correcting the tension values with the OL-SRC: this curve always establishes the link between the adaptation and ST outputs, in CL as in OL. (Actually our linearized OL-SRC would be the right choice, but there is only a slight difference between it and the OL-SRC for which we have an analytical expression). For example, in OL, at $t = 0$ $A_{imax} = 37.8\%$ corresponds to a 7 dB adaptation output (this of course for a 7 dB step input). In steady-state (Fig. 8) $A(\infty) = 8.48\%$ corresponding to 1.21 dB, giving exactly the right $A(0)/A(\infty)$ ratio (5.79).

Midway, at 4.10 dB (giving 22.3% tension) one reads off $t_{1/2} \approx 6.3$ s, which is close to the expected value of 6.1 s.

Without correcting with the OL-SRC and associating $t_{1/2}$ to the ST output halfway between 37.8% and (37.8/5.79)%, one also finds $t_{1/2} \approx 6.3$ s. Why then this tedious correction? It becomes necessary at intensities out of the linear range of the OL-SRC. Figure 9 shows the 75% response to a 16.6 dB input in OL and 24 dB input in CL. In OL, without correction $t_{1/2} \approx 8.75$ s instead of 6.1 (and this corresponds to 11.0 s when measured as in the literature, at 50% corresponding to 37.5%). Without correction, half-lives appear longer at high intensity. We shall return to this important point in the discussion.

These conclusions are equally valid in CL. At 10 dB (Fig. 8) $t_{1/2} \approx 7.2$ s with or without correction, and at 24 dB (Fig. 9) $t_{1/2} \approx 11.0$ s without correction instead of 7.2 s. Notice that the corrected values do not correspond to the expected half-life of 8.8 s ($\tau = 12.7$ s).

If we replace the ST model with a static nonlinearity in the form of the third degree polynomial we used to fit the OL-SRC, we obtain the same behavior. This makes sense intuitively because the muscle dynamics are very fast and thus hardly influence adaptation. We conclude that the nonlinear SRC is responsible for the 7.2–8.8 discrepancy.

Upon closer look, the process is not exactly exponential because the feedback to the adaptation is not proportional to its output but filtered by the
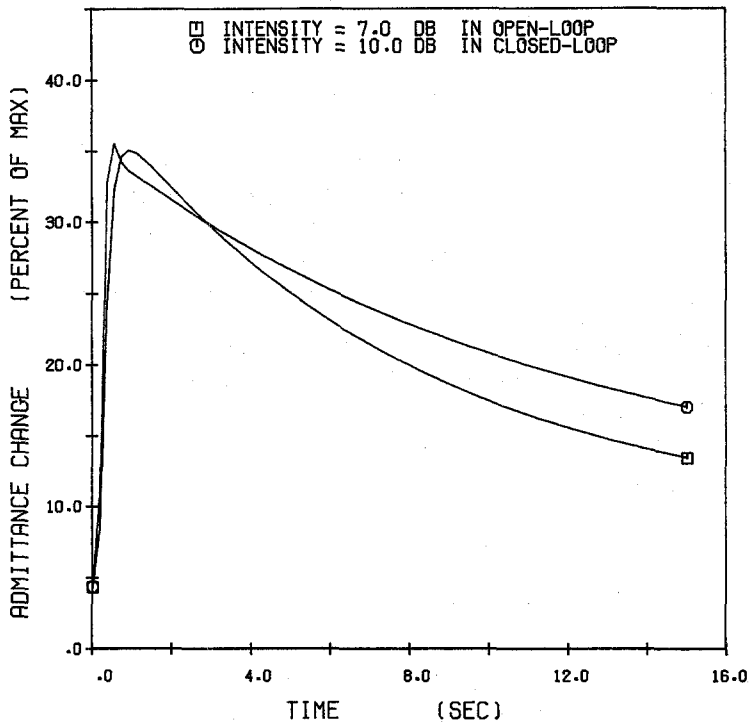
Fig. 8. Response of the complete AR model to a 10 dB step (CL) and a 7 dB step (OL) (both in linear region of SRC)
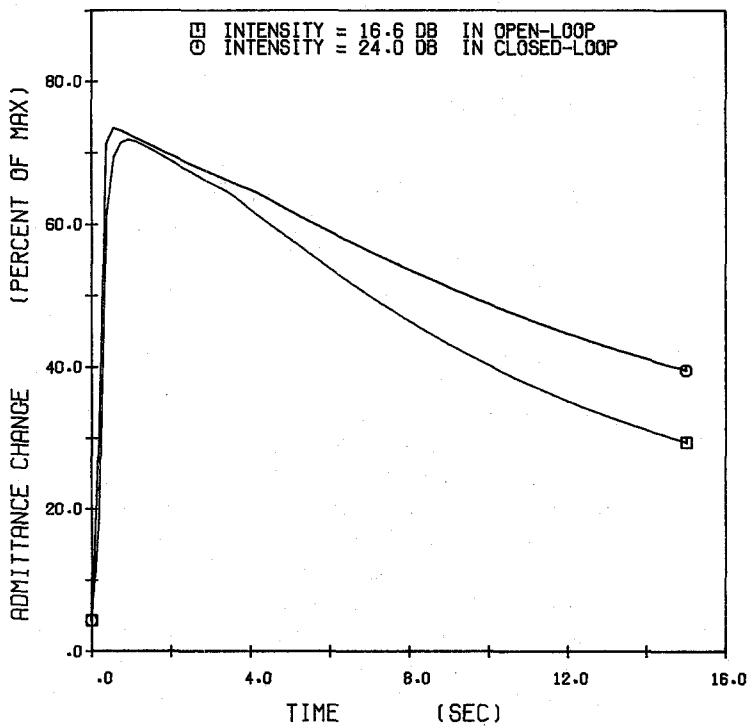
Fig. 9. Response of the complete AR model to a 24 dB step (CL) and a 16.6 dB step (OL)

nonlinear SRC. We can only measure a pseudo half-life in CL. In fact, for 10 dB (as in Fig. 8), a 100 s simulation revealed a 1.56 dB steady state (obtained by correcting the output with the OL-SRC) instead of 1.75 dB (7/4).

This corresponds to a pseudo half-life of 7.5 s, again inferior to 8.8 s.

Adaptation outputs is intrinsically exponential (for step inputs). This is also true in the whole reflex model

in OL; in CL, it is true only for a constant SRC slope, not for the real sigmoidal SRC.

We keep our calibration as it stands because it illustrates the effect of feedback on τ_a and gives values close to the expected ones.

4.4 Calibration of the Recovery Process

From the piecewise linear model in 3.3,

$$\tau_{\text{rec}} = \tau_a/(1 + MG_0) = P_{1\,(\text{off})}/(1 + MG_0)\,, \qquad (20)$$

where we distinguish between $P_{1\,(\text{off})}$ and $P_{1\,(\text{on})} = 50.8\,\text{s}$ determined in Sect. 4.3. Since $\tau_{\text{rec}} = 360$ ms, $P_{1\,(\text{off})} = 0.36(1 + MG_0) = 2.26$ and $k = 50.8 - 2.26 = 48.5$ so that

$$P_1 = 2.26 + 48.5\,(F_{\text{on off}})\,. \qquad (21)$$

The negative output of this process is forced to zero by the MU thresholds.

5 Simulations

Referring to Fig. 4, we can write down the equations of the model (we have included a mechanical coupling transfer function – see discussion). In the Laplace domain we have

$$E = I - G_R S\,, \qquad (22)$$

$$X = H_{\text{som}} E\,, \qquad (23)$$

$$X_{\text{ad}} = H_{\text{ad}} X = (G_0^{-1} + G_{\text{ad}})^{-1} X\,, \qquad (24)$$

$$YTHR_i(s) = THR_i[X_{\text{ad}}]\,, \qquad (25)$$

$$YSAT_i(s) = SAT_i[YTHR_i(s)]\,, \qquad (26)$$

$$Z_i = YSAT_i(s)F_i\,, \qquad (27)$$

$$ZTOT = \sum_{i=1}^{40} Z_i\,, \qquad (28)$$

$$ZTEND = H_{\text{tend}} ZTOT\,, \qquad (29)$$

$$S = ZTEND(\exp - s\tau_D)\,, \qquad (30)$$

$$H_{\text{som}} = 1/(1 + s\tau_s)\,, \qquad (31)$$

$$G_{\text{ad}} = M/(1 + s\tau_a)\,, \qquad (32)$$

$$H_{\text{ad}} = G_0(1 + s\tau_a)/(1 + MG_0 + s\tau_a)\,. \qquad (33)$$

Defining $YTHR_i$ and $YSAT_i$ respectively as the threshold and saturation operators acting on a function, we can write the global time domain equations:

$$s(t) = \int_0^{t-\tau_D} h_{\text{tend}}(t-x-\tau_D) \sum_{i=1}^{40} \int_0^x g_i(\tau)d\tau\, YSAT_i$$

$$\cdot \left\{ YTHR_1 \cdot \left[\int_0^{x-\tau} h_{\text{som}}(x-\tau-\alpha)\left[i(\alpha) - G_R s(\alpha)\right] \right. \right.$$

$$\left. \left. \cdot d\alpha - \int_0^{x-\tau} g_{\text{ad}}(x-\tau-t')x_{\text{ad}}(t')dt' \right] \right\} dx\,, \qquad (34)$$

$$x_{\text{ad}}(t) = \int_0^t h_{\text{som}}(t-\tau)\left[i(\tau) - G_R s(\tau)\right]$$

$$\cdot d\tau - \int_0^t g_{\text{ad}}(t-\tau)x_{\text{ad}}(\tau)d\tau\,. \qquad (35)$$

The system appears as two nonlinear coupled integral equations with input dependent parameters. These were simulated on a IBM SYS-370 using the Continuous System Modeling Program CSMP III, which seemed the most appropriate to treat the nonlinearities and reveal the fine structure of MU recruitment. We found the fix step 4th order Runge-Kutta algorithm to be faster than the more indicated Stiff method. We shortened the step-size around the input discontinuities.

6 Discussion

6.1 General Discussion

Our model seems to combine enough ingredients to reproduce the fundamental behaviors of the AR at 2000 Hz. In CL, T_{lat} falls from 0.17 s to 0.14 s and TS from 0.65 s to 0.56 s when the intensity increases from 4 to 24 dB (Fig. 10B). The same behavior is observed in OL (Fig. 10A), a property related to the distributed nature of the parallel pathways.

Feedback is seen to accelerate the response and to decrease A_{imax}. At high frequencies, the overdamped response is the result of two synergetic effects: a low feedback gain and a rapid adaptation (we shall see further that the two are related). Figure 11 illustrates the oscillations produced in CL when the feedback gain is raised to $G = 2$.

For intensities going from 4 to 24 dB, T_{rel} drops from 660 to 460 ms while T_{rise} varies from 260 to 170 ms, which properly simulated URS (see Sect. 2).

Our value of TS (0.6 s) is low compared to 2.7 s reported by Wilson et al. (1984) at 2000 Hz (even though their standard deviations is 90%). This is probably due to the absence of mechanical coupling (at the tendon). We have found that by assigning a 400 ms time constant to a first order system simulating this coupling (Inbar and Ginat 1983), TS can be well over 1 s, without a significant influence on adaptation and recovery. It is interesting to notice that such a time constant would make the ST the slowest component of the AR, the one which determines the low frequency response (cutoff ≈ 7 Hz – see Sect. 2).

The rigid calibration procedure at 2000 Hz may appear as a major shortcoming if one wishes to extend the model to other stimuli. The efforts is warranted when precise intensity dependent effects are the object of study. For another stimulus, a new calibration of the force levels in decibels would have to be done with the

OPEN-LOOP RESPONSE TO A 1.0 SEC PULSE
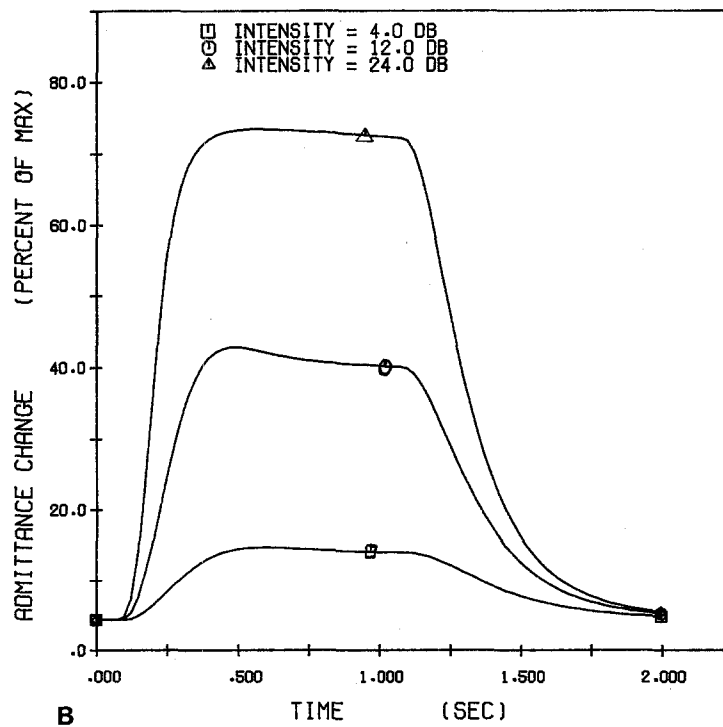

A
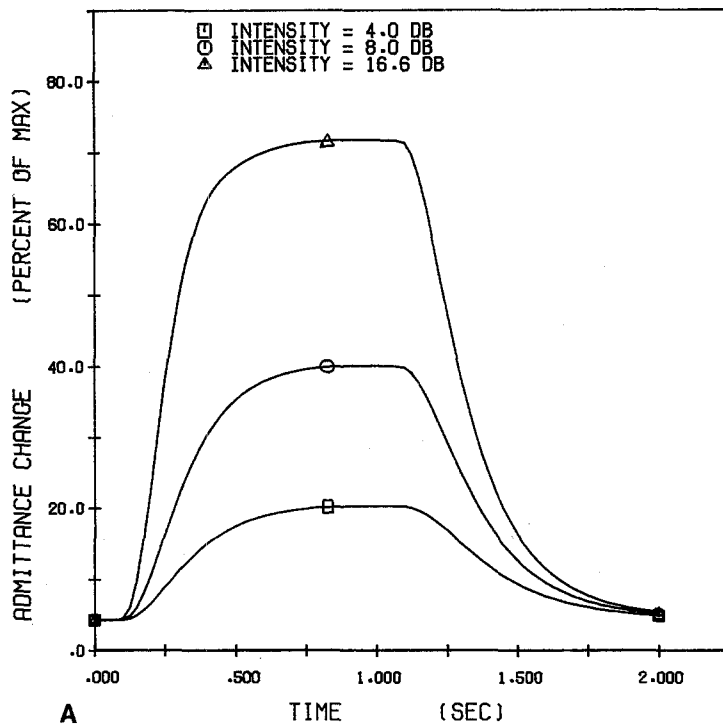
CLOSED-LOOP RESPONSE TO A 1.0 SEC PULSE

B

Fig. 10A, B. AR response to a 1-s pulse at different intensities to compare T_{lat}, TS and T_{rel}.
A Open-loop: Intensity = 4.0, 8.0, and 16.6 dB.
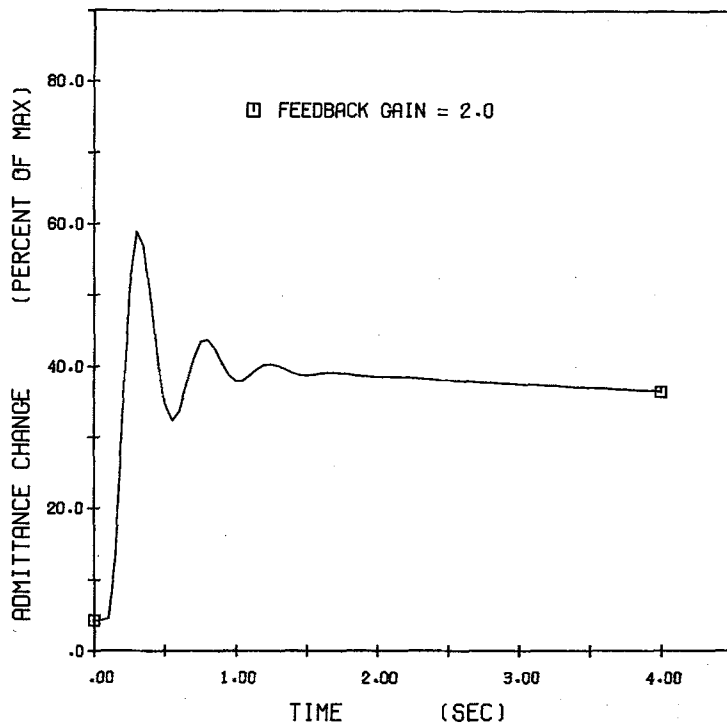**B** Closed-loop: Intensity = 4.0, 12.0, and 24.0 dB

338

Fig. 11. Closed-loop response with a high feedback gain. $G = 2.0$, intensity $= 24 \, \text{dB}$

corresponding SRC; however the recruitment levels in grams would remain unchanged, because they are a property of the stapedius.

6.2 Discussion of the Adaptation Model

Ignoring the precise site and mechanism of adaptation we chose to model it by a linear system in which there is no noise (zero input entails zero output). However, the first MU recruits at 0.854 g $(F_{t1} = Bg_1)$, a level we assume is produced by noise or rest tonus. We remark that this is also the case in the SRC; for example, in Wilson and McBride (1978), the admittance change is 3.7% at ART.

In Sect. 4.3, it was shown that the higher the feedback gain, the longer the time constant of adaptation. This is conceivable intuitively since negative feedback opposes output variations. Our calculations predict that the adaptation time constant in open-loop is 6–7 s at 2000 Hz, with a ratio $A(0)/A(\infty) \approx 5.8$.

It is known (e.g. Wilson et al. 1984) that τ_a in CL increases when stimulus frequency decreases. Also, τ_a is proportional to the feedback gain. Since feedback gain is higher at low frequencies, we conclude from our model that *the frequency dependence of the adaptation time constant is due to the frequency dependence of the feedback gain, a property of the middle ear, and is not a property of the neural circuits responsible for adaptation.*

This would require either that the process is 1) the same in every afferent frequency specific pathway or 2) located at a level where frequency is no more encoded. However we know (Sect. 2) that the adapted response can be revived by a change of frequency; this fact lends support to the first possibility.

Experimental data agree on the intensity independence of τ_a and $A(0)/A(\infty)$ below 2000 Hz. Our simulations show however that without correcting with the OL-SRC, τ_a increases at higher intensity [and $A(0)/A(\infty)$ decreases], be it in OL or in CL. This may explain the intensity dependence reported in the literature at frequencies below 2000 Hz and the ambiguity in the 2000–4000 Hz range. Referring to Fig. 12 and reasoning in OL, we see the exponential adaptation filtered by the OL-SRC. The output is obviously not exponential. Let us consider the linearized OL-SRC used for our simulation (Fig. 12C). The adaptation output $R(0)$ is converted to a tension $F(0)$. In steady state, $R(\infty) = R(0)/5.79$ produces $F(\infty)$. If the tangent at $(R(0), F(0))$ is taken as the real SRC, the asymptotic force is $F'(\infty)$. Knowing the equation of this tangent, one could deduce the correct values of τ_a and of $R(0)/R(\infty)$.

But the slope changes, and $F'(\infty)$ decreases so the exponential is scaled differently as time goes on. The effect on uncorrected measurements (or on the $t_{50\%}$ reported in the literature) is an increase of τ_a with intensity. This appears clearly and somewhat artificially in Fig. 9 where one sees the change in
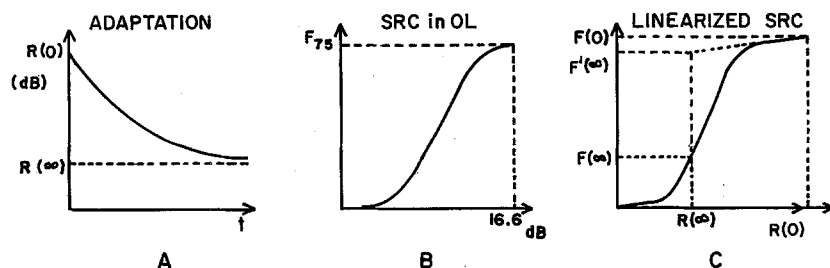
Fig. 12A–C. Intensity dependence of adaptation rate. $R(t)$ refers to the adaptation output in db at time t, and $F(t)$ refers to the corresponding tension. **A** Output of adaptation process. **B** Open-loop SRC. **C** Linearized version of the OL-SRC

scaling when the 39th MU drops out at 64%; in fact the rate-coding $S_{39} = 0.508$, while $S_{38} = 0.857$. The effect is visible at 2000 Hz because in the range of study our SRC is nonlinear. It should be even more pronounced at low frequencies where the saturation of the response occurs earlier.

Our second conclusion is the following: *the sigmoidal SRC is responsible for the more sustained response (longer τ_a) at high intensities and low frequencies.* Of course our conclusions are contingent on the choice of a linear system exhibiting an exponential step response for adaptation. A nonlinear model could also account for the behaviors. For example, it may be that the AR has MUs for which τ_a varies inversely with recruitment level. The model we have chosen is referred to as a "self inhibitory feedback current model" by Zeevi and Bruckstein (1981) in which an electrogenic Na$^+$ pump generates a self inhibitory current, producing slow adaptation transients (see also Fohlmeister 1979).

Another possibility is a feedforward model as used by Semmlow and Chen (1977) to account for the

pupillary escape and capture. This more complicated model uses low gain feedforward pathways short-circuiting the adaptation processes (slow and fast). They relate this bypass to crosstalk between the pathways. One cannot refute the plausibility of such a process in view of the complexity of the neural circuitry involved.

6.3 Discussion of the Recovery Model

The mechanisms governing recovery are even more obscure than those responsible for adaptation. The striking feature of recovery is its speed, a property none of the models studied could reproduce. We have assumed that recovery does not affect the adaptative phase, but they are probably intertwined. It may be that adaptation is faster than recovery, as in cochlear neurons, but that it is slowed down by another process. This question cannot be resolved by our model. It is possible, as Borg and Ödman have pointed out (1979), that adaptation and recovery balance each other out
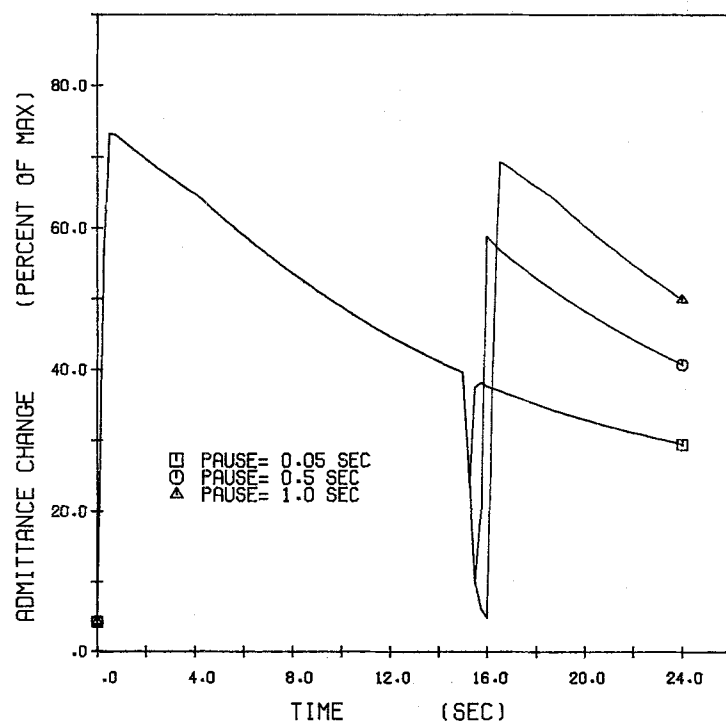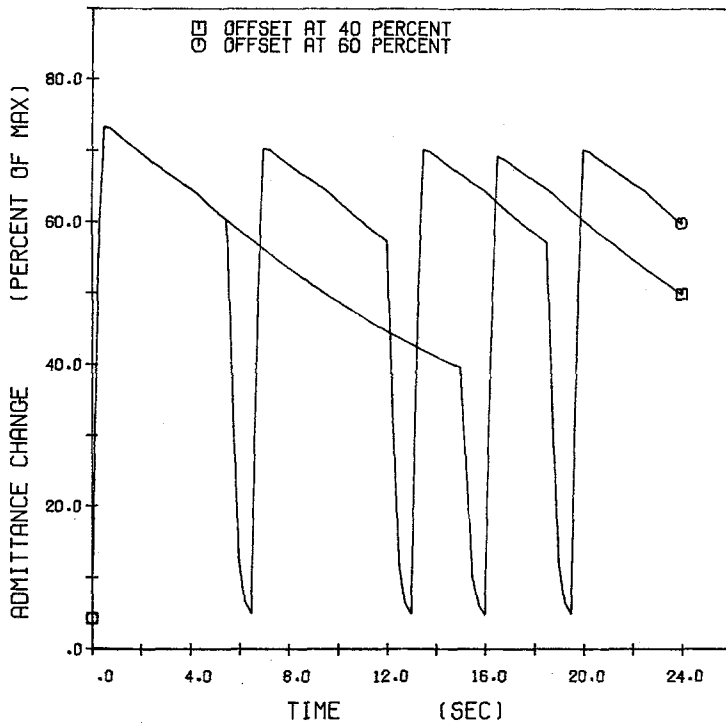

Fig. 13. AR recovery to a silence period of 50, 500 and 1000 ms. Intensity = 24 dB (CL). Offset occurs at 40% (or at $t = 15$ s)

Fig. 14. AR recovery from a one second pause to show the influence of preoffset level. Intensity = 24 dB (CL). Pause occurs at 60% and at 40%. Notice the recovery stabilizes quickly (within 2 pauses) to a fixed value in the 60% case

partially, but are based on different mechanisms operating in separate sites.

The negative values are problematic, and refinements towards nonlinear models are certainly needed. However, our main concern is the presence of a memory of the last onset, even though the output is shorted to zero at offset.

The exponential memory determines the level that the response to the next onset B_{imax} will reach. It should equal A_{imax} if the silence lasts many recovery time constants. This is illustrated in Fig. 13 where pauses of different lengths occur at 40% (as in Borg and Ödman 1979). Figure 14 compares recovery with a 1-s pause at 60% ($t = 5.5$ s) and 40% ($t = 15$ s). It is nearly the same in both cases, meaning it is almost independent of preoffset level when the silence is long enough.

Finally, we notice on the 60% curve of Fig. 14 that recovery becomes quite rapidly constant (within 2 pauses) and that a stimulus with periodic silent intervals does produce a more sustained response.

7 Conclusion

Our model of the AR in man has been developed to properly account for the open-loop and closet-loop nonlinearities at 2000 Hz in order to study the adaptation nonlinearities. The parameter distribution to the parallel pathways in accordance with Henneman's size principle and the relations of Milner-Brown et al. produced a staircase recruitment of the ST MUs resulting in a piecewise linearization of the OL-SRC.

The key factor in the calibration was the opening of the feedback loop with Borg's 0.3 dB/dB regulation value.

Our analysis permitted us to explain two adaptation nonlinearities, within the hypothesis of a linear system to model it: the frequency and intensity dependence of the adaptation rate, manifestations respectively of the frequency dependence of the feedback gain and of the sigmoidal SRC.

Open-loop measurements are highly indicated to verify the model predictions relative to the frequency independence of the open-loop adaptation rate. We could verify this by redoing our calibration at 500 Hz for example, and verifying whether the same constant $\tau_a \approx 6\text{--}7$ s can account for the slow closed-loop adaptation rate.

We must insist on the importance of knowing the asymptotic activity and the SRC to characterize central processes of the arc such as adaptation. There is a large gap between our way of measuring adaptation rate (or pseudo half-life in CL) and the methods reported in the literature. In fact, a prime motivation of this work has been to sensitize clinicians to the physical quantities relevant in the modeling context. We remain aware, however, of such practical difficulties as the large variability and drift in the results, of the complications involved in the determination of an asymptotic response, etc.

It may turn out that only a macroscopic description of the neural activity of adaptation and recovery, based on sound neurophysiological evidence, will eventually elucidate their mechanisms. We hope the

"experiments" conducted on this model will suggest new experimental procedures while stimulating further theoretical studies.

List of Abbreviations

ART: Acoustic reflex
BBN: Broadband noise
CL: Closed-loop
CNS: Central nervous system
CSMP: Continuous system modeling program
EMG: Electromyogram
FDI: First dorsal interosseous
MU: Motor unit
OL: Open-loop
SPL: Sound pressure level
SRC: Stimulus-response curve
ST: Stapedius
TS: Summation time
URS: Unidirectional rate sensitivity

References

American National Standards Institute (ANSI). American national standard specifications for aural acoustic immittance instruments. ANSI S 3.60 New York (1982)

Antablin J, Lilly D, Wilson R (1980) Intra-subject variability of acoustic reflex adaptation in normal listeners. American Speech-Language-Hearing Association Convention. Detroit, Michigan

Blevins CE (1964) Studies on the innervation of the stapedius muscle of the cat. Anat Rec 149:157–172

Blevins CE (1967) Innervation patterns of human stapedius muscle. Arch Otolaryngol 87:30–36

Blevins CE (1968) Motor units in the stapedius muscle. Arch Otolaryngol 87:47–52

Borg E (1968) A quantitative study of the effect of the acoustic stapedius reflex on sound transmission through the middle ear of man. Acta Otolaryngol 66:461–472

Borg E (1971) Regulation of middle ear sound transmission in the nonanesthetized rabbit. Acta Physiol Scand 86:175–190

Borg E (1972) The dynamic properties of the acoustic middle ear reflex in nonanesthetized rabbits. Quantitative aspects of a polysynaptic reflex system. Acta Physiol Scand 86:366–387

Borg E (1973a) On the neural organization of the acoustic middle ear reflex. A physiological and anatomical study. Brain Res 49:101–123

Borg E (1973b) Nonlinear dynamic properties of a somatomotor reflex system. A model study. Acta Physiol Scand 87:15–26

Borg E (1976) Neurophysiology of the acoustic stapedius reflex. Proceedings of the Third International Symposium on Impedance Audiometry 6–11

Borg E, Møller AR (1968) The acoustic middle-ear reflex in unanesthetized rabbits. Acta Otolaryngol 65:575–585

Borg E, Nilsson R (1984) Acoustic reflex in industrial noise. In: Silman S (ed) The acoustic reflex. Academic Press, Orlando

Borg E, Ödman B (1979) Decay and recovery of the acoustic stapedius reflex in humans. Acta Otolaryngol 87:421–428

Borg E, Counter SA, Rösler G (1984) Theories of middle-ear muscle function. In: Silman S (ed) The acoustic reflex. Academic Press, Orlando

Christakos CN (1982a) A linear stochastic model of the single motor unit. Biol Cybern 44:79–89

Christakos CN (1982b) A study of the muscle force waveform using a population stochastic model of skeletal muscle. Biol Cybern 44:91–106

Clynes M (1962) The nonlinear biological dynamics of unidirectional rate sensitivity illustrated by analog computer analysis, pupillary reflex to light and sound, and heart rate behavior. Ann NY, Acad Sci 98:806–845

Dallos PJ (1964) Study of the acoustic reflex feedback loop. IEEE Trans BME-11:2–7

Dallos PJ (1973) The auditory periphery. Biophysics and physiology. Academic Press, New York London

Duifhuis H, Bezemer AW (1983) Peripheral auditory adaptation and forward masking. In: Klinke R, Hartmann R (eds) Hearing – Physiological bases and psychophysics. Springer, Berlin Heidelberg New York

Eggermont JJ (1975) Cochlear adaptation: a theoretical description. Biol Cybern 19:181–189

Fisch U, Schulthess GV (1963) Electromyographic studies on the human stapedial muscle. Acta Otolaryngol 56:287–297

Fohlmeister J (1979) A theoretical study of neural adaptation and transient responses due to inhibitory feedback. Bull Math Biol 41:257–282

Henneman E (1981) Recruitment of motoneurons: the size principle. In: Desmedt JE (ed) Motor unit types, recruitment and plasticity in health and disease. Karger, Basel

Henneman E, Somjen G, Carpenter DO (1965) Excitability and inhibility of motoneurons of different sizes. J Neurophysiol 28:599–620

Hétu R, Carreau P-U (1977) Decay of the acoustic reflex during steady-state and intermittent noise exposures. J Acoust Soc Am Suppl 1:61, S3

Holden AV (1976) Models of the stochastic activity of neurons. Lecture notes in biomathematics, vol 12. Springer, Berlin Heidelberg New York

Inbar GF, Ginat T (1983) Effects of muscle model parameter dispersion and multiloop segmental interaction on the neuromuscular system performance. Biol Cybern 48:69–83

Lalande N, Hétu R (1979) The influence of the period and the duty cycle of an intermittent noise on the acoustic reflex activity. J Acoust Soc Am (Abstract)

Lutman ME, Martin AM (1978) Adaptation of the acoustic reflex to combinations of steady-state and repeated pulse stimuli. J Sound Vibr 56:137–150

Lyon MJ, Malmgern LT (1982) A histochemical characterization of muscle-fiber types in the middle-ear muscles of the cat. I. The stapedius muscle. Acta Otolaryngol 94:99–109

Mayrand N (1982) Etude des déterminants physiques de la réponse temporelle du réflexe acoustique sollicité par un bruit à large bande de fréquences. Thèse de doctorat, Université de Montréal

Milner-Brown HS, Stein RB, Yemm R (1973) The orderly recruitment of human motor units during voluntary isometric contraction. J Physiol 230:359–370

Møller AR (1961) Network model of the middle ear. J Acoust Soc Am 33:168–176

Møller AR (1962) Acoustic reflex in man. J Acoust Soc Am 35:1526–1534

342

Schroeder MR, Hall JL (1974) Model for mechanical to neural transduction in the auditory receptor. J Acoust Soc Am 55:1055–1060

Semmlow JL, Chen DC (1977) A simulation model of the human pupil light reflex. Math Biosci 33:5–24

Silman S (1984) The acoustic reflex. Academic Press, Orlando

Smith RL, Brachman ML (1982) Adaptation in auditory-nerve fibers: a revised model. Biol Cybern 44:107–120

Stark L (1959) Stability, oscillations and noise in the human pupil servo-mechanism. Proc IRE 47:1925–1939

Teig E (1972a) Force and contraction velocity of the middle-ear muscles in the cat and the rabbit. Acta Physiol Scand 84:1–10

Teig E (1972b) Tension and contraction time of motor units of the middle-ear muscles in the cat. Acta Physiol Scand 84:11–21

Teig E, Dahl HA (1972) Actomyosin ATPase activity of middle-ear muscles in the cat. Histochemie 29:1–7

Tietze G (1969a) Zum Zeitverhalten des akustischen Reflexes bei Reizung mit Dauertönen. Arch Klin Exp Ohren-Nasen-Kehlkopfheilkd 193:43–52

Tietze G (1969b) Einige Eigenschaften des akustischen Reflexes bei Reizung mit Tonimpulsen. Arch Klin Exp Ohren-Nasen-Kehlkopfheilkd 193:53–69

Wilson RH, McBride LM (1978) Threshold and growth of the acoustic reflex. J Acoust Soc Am 63:147–154

Wilson RH, McCullough JK, Lilly DJ (1984) Acoustic-reflex adaptation: morphology and half-life data for subjects with normal hearing. J Speech Hear Res 27:586–595

Wilson RH, Steckler JK, Jones HC (1978) Adaptation of the acoustic reflex. J Acoust Soc Am 64:782–791

Zeevi YY, Bruckstein AM (1981) Adaptative neural encoder model with self-inhibition and threshold control. Biol Cybern 40:79–92

Zwislocki J (1960) Theory of temporal auditory summation. J Acoust Soc Am 32:1046–1060

Dr. Jean-Robert Derome
Physics Department
University of Montreal
C.P. 6128 Succ. A
Montreal, Quebec H3C 3J7
Canada